Verification of net primary production estimation method in the Mongolian Plateau using Landsat ETM+ data

Yan XIONG[1], **Kanako MURAMATSU**[1], **Masahiro HIRATA**[2], **Kazato OISHI**[2], **Ichirow KAIHOTSU**[3], **Tamio TAKAMURA**[4], **Shinobu FURUMI**[1], **Noboru FUJIWARA**[1]

[1]**Nara Women's University,**[2]**Kyoto University,**[3]**Hiroshima University,**[4]**Chiba University**

ABSTRACT

We plan to estimate global net primary production (NPP) of vegetation using Advanced Earth Observing Satellite-II (ADEOS-II) Global Imager (GLI) multi-spectral data. We derived an NPP estimation algorithm from ground measurement data on temperate plants in Japan. From the algorithm, we estimated NPP using a vegetation index based on pattern decomposition ($VIPD$) for the Mongolian Plateau. The $VIPD$ was derived from Landsat ETM+ multi-spectral data, and the resulting NPP estimation was compared to ground data measured in a semi-arid area of Mongolia. The NPP estimation derived from satellite sensor data agreed with the ground measurement data within a 15% margin of error when all above-ground vegetation NPP was calculated for different vegetation classifications.

KEY WORDS: NPP, reflectance, photosynthesis, canopy structure

1 INTRODUCTION

The release of greenhouse gasses such as carbon dioxide may cause global warming. On land, only photosynthesis by vegetation can naturally absorb carbon dioxide. Net primary production (NPP) represents the net new carbon stored as biomass in the stems, leaves, or roots of vegetation. This stored carbon is an important part of the carbon cycle. By studying carbon dioxide absorption by vegetation, we can better understand the mechanisms of global warming.

Satellite sensors allow for global NPP estimates and the monitoring of NPP anywhere in the world. At present, satellite data are commonly used to estimate the normalized difference vegetation index (NDVI). NDVI uses only two reflectance channels, visible and near-infrared (VNIR). However, many satellites now carry sensors that detect multi-spectral bands. For example, Japan's National Space Development Agency (NASDA) launched the Advanced Earth Observing Satellite-II (ADEOS-II) on December 14, 2002. The satellite's five sensors include a multi-spectral sensor global imager (GLI).

To use multi-spectral satellite sensor data effectively, we developed a new vegetation index, $VIPD$, based on the pattern decomposition method (Fujiwara et al. 1996, Furumi et al. 1998, Hayashi et al. 1998, Muramatsu et al. 1998, Daigo et al. in press) and examined the relationship between $VIPD$ and NPP. We are currently developing an algorithm to estimate global NPP using multi-spectral satellite sensor data such as ADEOS-II GLI data. The algorithm is based on temperate plant leaf and canopy measurements taken in Japan (Furumi et al. submitted).

For global NPP mapping, we must validate the NPP estimation for a wide range of vegetation densities. We selected a Mongolian site to validate estimation in conditions of low vegetation density. The vast, flat Mongolian Plateau makes an ideal site for verifying the NPP estimation from satellite sensor data. Moreover, the site has also been used by the ADEOS-II/AMPEX-AMSR/AMSR-E project to verify soil moisture estimates (Kaihotsu 2000). For that project, ground measurements of vegetation biomass and NPP were included with the ground measurements of soil moisture.

In this study, we used multi-spectral Landsat ETM+ data to estimate the NPP. We then compared the estimation result to ground measurement data from the Mongolian Plateau.

2 STUDY AREA AND NPP GROUND MEASUREMENT

This section describes the Mongolian Plateau study site and the results of NPP ground measurements.

2.1 Study Area

The size of the study area (Figure 1) is $60km \times 60km$, where lies on northeast of Mandalgovi and 235 km south-southwest of Mongolia's capital, Ulaanbaatar.

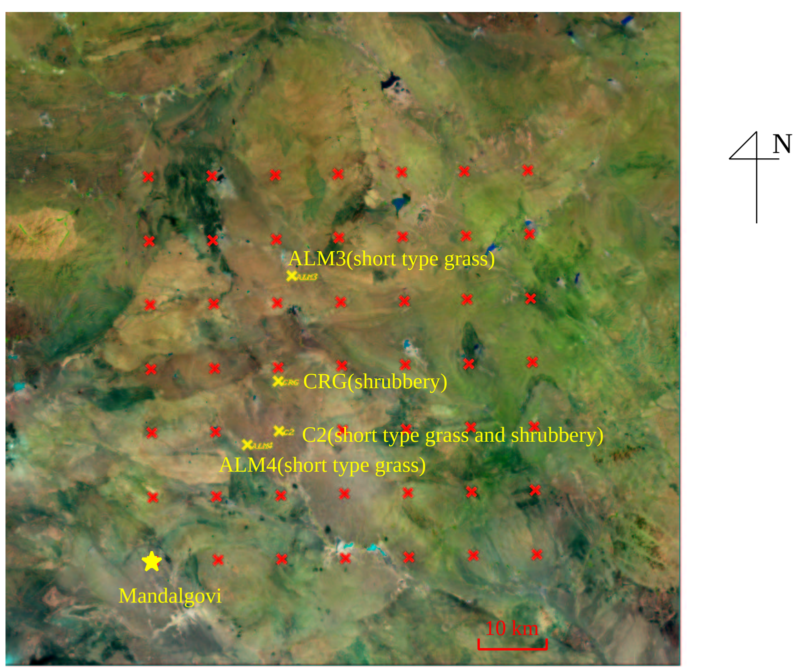

Figure 1. Mandalgovi, Mongolia study area. Yellow crosses indicate NPP measurement points in 2001. Red crosses show ground observation points observed in synchrony with scheduled fly-over dates of Aqua or ADEOS-II satellites. The red crosses have an interval distance of 10 km.

The four yellow crosses in Figure 1 indicate NPP measurement sites. We took measurements from April to October 2001. Areas ALM3 and ALM4 consist mainly of short grass, area CRG features shrubbery, and area C2 has intermingled short grass and shrubbery. The red crosses indicate ground observation sites for data such as vegetation biomass and soil moisture. Measurements were made in synchrony with Aqua or ADEOS-II satellite fly-over times. The red crosses have an interval distance of 10 km.

2.2 NPP Ground Measurement

To coordinate with satellite sensor data, NPP was measured at four uniform areas. We measured the latitude and longitude at the NPP ground observation points using World Geodetic System 1984 (WGS84) GPS equipment (GARMIN-III GPSplus, GARMIN), as detailed in Table 1. As the study area is used for pastureland, livestock or other animals may eat the vegetation, so we erected a fence around the plot in which we measured the gross production of vegetation. One time every month, we cut the plant biomass at ground level in the enclosed area more than two repetition and measured the above-ground plant growth. The collected plants were oven dried (at 130°C for two hours) to measure the dry weight. The following equation (1) was used for converting the organic dry matter weight into a carbon dioxide value:

$$C_6H_{12}O_6 : 6\ CO_2 = 30 : 44 \tag{1}$$

We measured NPP from April to October 2001 and from June to August 2002. Table 1 shows the NPP ground measurement data for June 2001. We compared the June 2001 ground measurement data to the June 2001 Landsat ETM+ data.

We assumed an approximately 2:1 ratio of above-ground to underground plant growth (Kitamura 1973, Rarcher 1975), as shown in equation (2). For different types of vegetation, the estimation error for underground growth nears ±15% of the entire plant value (including above-ground and underground growth).

$$Above\ ground\ part\ NPP\ :\ Underground\ part\ NPP\ =\ 2 : (1 \pm 0.45) \tag{2}$$

Table 1. NPP measured at four points on the Mongolian Plateau in June 2001.

Points name	(Latitude, Longitude)	NPP ground measurement data $[kgCO_2/(m^2 \cdot month)]$ Above-ground part	Whole plant
ALM3	(N46°08'28.3",E106°33'10.7")	0.039	0.059±0.009
CRG	(N45°59'37.5",E106°31'15.2")	0.018	0.027±0.004
C2	(N45°55'22.5",E106°31'21.2")	0.020	0.030±0.005
ALM4	(N45°54'17.2",E106°27'25.4")	0.018	0.027±0.004

NPP measurement values for the above-ground part of the plant were 0.039, 0.018, 0.020, and 0.018 $[kgCO_2/(m^2 \cdot month)]$ at points ALM3, CRG, C2, and ALM4, respectively. The NPP for the whole plant was 0.059±0.008, 0.027±0.004, 0.030±0.004, and 0.027±0.004 $[kgCO_2/(m^2 \cdot month)]$ at points ALM3, CRG, C2, and ALM4, respectively. Table 1 summarizes the results. The results were used to verify the NPP estimation derived from satellite data. Verification methods are described in the next section.

3 METHOD:ESTIMATING NPP FROM SATELLITE DATA

This section discusses the method of determining NPP from $VIPD$ calculated from satellite reflectance data. Section 3.1 details the $VIPD$ calculation; section 3.2 presents the general formula for NPP; and section 3.3 describes the relationship of $VIPD$ and photosynthesis or NPP established using ground measurement data from temperate plants in Japan.

3.1 Pattern Decomposition Method And VIPD

The pattern decomposition method is used to analyze multi-spectral reflectance data (Fujiwara et al. 1996, Muramatsu et al. 1998, Daigo et al. in press). Any pixel (A_i) of satellite spectral reflectance data can be decomposed into three basic patterns: water, vegetation, and soil. The following equation (3) illustrates the conversion process:

$$A_i \rightarrow C_w P_{iw} + C_v P_{iv} + C_s P_{is} \tag{3}$$

Here, i corresponds to the wavelength bands. C_w, C_v, and C_s are the decomposition coefficients of water, vegetation, and soil, respectively. P_{iw}, P_{iv}, and P_{is} are the basic patterns of water, vegetation, and soil, given as follows:

$$\begin{aligned} Water\ pattern &= (P_{1w}, P_{2w}, ..., P_{nw}) \\ Vegetation\ pattern &= (P_{1v}, P_{2v}, ..., P_{nv}) \\ Soil\ pattern &= (P_{1s}, P_{2s}, ..., P_{ns}) \end{aligned} \tag{4}$$

where n is the number of wavelength bands from visible to short-wave infrared. For Landsat ETM+ data, n equals six (bands 1-5 and band 7).

The sum of the standard pattern for every band is 1 for normalization, as shown in equation (5). The decomposition coefficients C_w, C_v and C_s are found using least-square techniques.

$$\Sigma_{i=1}^{6} P_{il} = 1 \qquad (l = w, v, s) \tag{5}$$

This study used the $VIPD$ (Furumi et al. 1998 and Hayashi et al. 1998) determined by equation (6).

$$VIPD = \frac{C_v - C_s - \frac{S_s}{\Sigma_{i=1}^{6} A_i} C_w + S_s}{S_v + S_s} \tag{6}$$

where S_v and S_s are the sum of the reflectance of all bands for standard vegetation and soil, respectively, for all typical samples.

When vegetation is alive, $VIPD$ will near a value of one; when vegetation dies, $VIPD$ nears zero. $VIPD$ should also be approximately zero for water and soil. In general, the S_v and the S_s are constants; they express the reflective intensity of 100% of the vegetation and 100% of the soil, respectively. To investigate VIPD in detail, the reflective intensity of the vegetation and the soil contained in the pixel should be known. For this study, the S_v was 1.61. This area of Mongolia has relatively little vegetation biomass. The background soil, however, has a strong reflective intensity, which differs for each pixel. To increase the accuracy of estimation, we calculated the S_s for a pure soil pixel by using Landsat ETM+ data from a non-vegetated period in early spring. These calculations yielded an S_s of 1.4.

3.2 General Formula For NPP

Subtracting vegetative respiration (R_d) from gross primary production (GPP) results in NPP as follows:

$$NPP = GPP - R_d \,. \tag{7}$$

Since we measured NPP in the Mongolian Plateau every month, we also estimated a monthly NPP $[kgCO_2/(m^2 \cdot month)]$. GPP $[kgCO_2/(m^2 \cdot month)]$ was expressed as follows:

$$GPP = \int_0^{month} P(PAR(t))dt \tag{8}$$

where t is time, $PAR(t)$ $[W/m^2]$ is photosynthetically active radiation, and $P(PAR(t))$ $[kgCO_2/(m^2 \cdot month)]$ is gross photosynthesis as a function of $PAR(t)$ $[W/m^2]$.

The study site had a simple grassy vegetation structure. Thus, vegetative respiration R_d $[kgCO_2/(m^2 \cdot month)]$ could be well approximated from monthly average air temperature $T[°C]$ (Chang 1968, Goward and Dye 1987, Monteith 1981) as follows:

$$R_d = \frac{7.825 + 1.145T\ [°C]}{100} \times GPP \tag{9}$$

3.3 Algorithm To Estimate Global NPP From Satellite Data

In a region of low photosynthetically active radiation (PAR), photosynthesis increases as PAR becomes stronger. When PAR increases to a certain point, photosynthesis reaches saturation. In this study, the photosynthesis $P(PAR(t))$ $[mgCO_2/(m^2 \cdot s)]$ was expressed as a function of $PAR(t)$ $[W/m^2]$ as follows:

$$P(PAR(t)) = \frac{P_{max} \times b \times PAR(t)}{1 + b \times PAR(t)} \tag{10}$$

where P_{max} $[mgCO_2/(m^2 \cdot s)]$ is the value of photosynthesis when PAR is infinite. The b plots as a curve. When b becomes large, an increase in PAR will rapidly lead to photosynthetic saturation.

For any single leaf or canopy, photosynthesis is a function of PAR and $VIPD$ as expressed approximately by the following equation (Furumi et al. submitted):

$$P(PAR(t),\ VIPD(t)) = \frac{VIPD(t)}{VIPD_{std}} \times P_{std}(PAR(t)) \tag{11}$$

where $P_{std}(PAR(t))$ is the photosynthetic curve of a standard sample and $VIPD_{std}$ is the $VIPD$ of a standard sample. For $P_{std}(PAR(t))$ and $VIPD_{std}$, the value of many single leaves are averaged (Furumi et al. submitted). Table 2 lists the $P_{std}(PAR(t))$ and the $VIPD_{std}$.

Table 2. Values of $VIPD_{std}$ and $P_{std}(PAR(t))$

$VIPD_{std}$	$P_{std}(PAR(t))$	
0.56	$P_{max} = 0.53\ [mgCO_2/(m^2 \cdot s)]$	$b = 0.027\ [m^2/W]$

4 SEMI-ARID AREA SINGLE LEAF PHOTOSYNTHESIS

The NPP estimation algorithm used for this study is based on ground measurement data from temperate plants in Japan. Here, we examine the equation's applicability (11) to single-leaf plants in a semi-arid area, the Mongolian Plateau.

Using a FieldSpec FR spectroradiometer (Analytical Spectral Devices, Inc.), we measured many single leaves and determined an average reflectance value from nine single leaves from *Caragana* shrubs found in the Mongolian Plateau in 2001 and 2002. Figure 2 lists the findings.

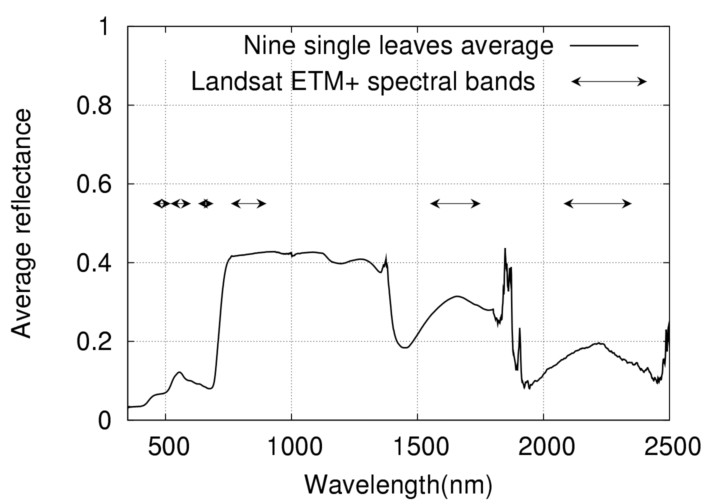

Figure 2. The average reflectance of nine *Caragana* leaves.

We also calculated the reflectance of the Landsat ETM+ spectral bands as shown in Figure 3. Using the reflectance, we calculated the $VIPD$ of a single leaf (Table 3).

Table 3. Average reflectance of nine leaves and $VIPD$ for the Mongolian Plateau.

	Landsat ETM+ bands						Vegetation index
	Band1	Band2	Band3	Band4	Band5	Band6	$VIPD$
Reflectance	0.077	0.116	0.071	0.445	0.290	0.145	0.49

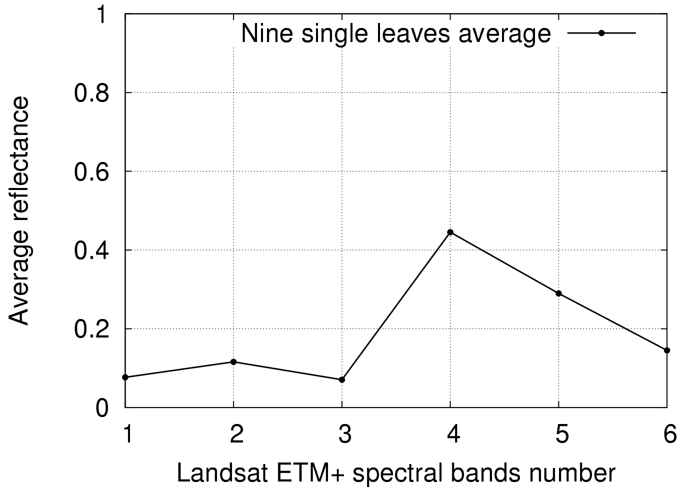

Figure 3. The average reflectance of Landsat ETM+ spectral bands

Using a CO_2 Analyzer LCA-4 (Analytical Development Co. Ltd.), we also measured light-response photosynthetic curves for many single leaves. Figure 4 shows the average *Caragana* leaf photosynthesis measured before noon and in afternoon. The vertical and horizontal error bars show the standard deviation of measured PAR and measured photosynthesis, determined as $\pm$ 23 $[W/m^2]$ and $\pm$ 0.07 $[mgCO_2/(m^2 \cdot s)]$, respectively. The photosynthetic curve $P(PAR(t))$ for a single leaf in the Mongolian Plateau was calculated using equation (11). The value agrees with the ground measurement data within allowable measurement error.

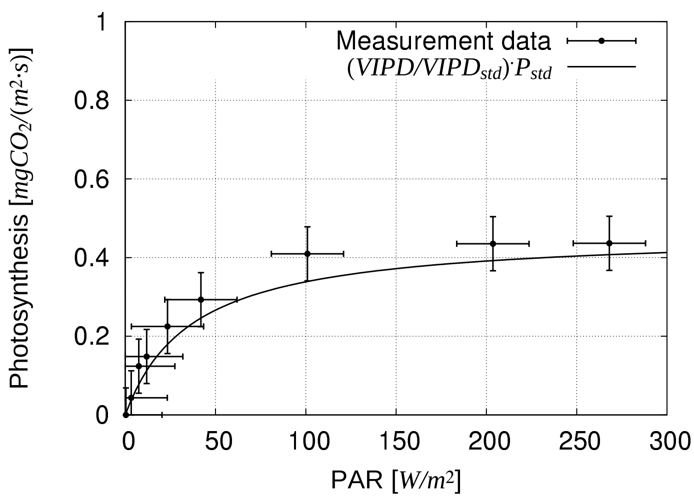

Figure 4. Ground measurement and estimation of photosynthesis.

5 NPP ESTIMATION USING LANDSAT ETM+ DATA

We estimated the NPP of the Mongolian Plateau study area using Landsat ETM+ data from June 12, 2001. The satellite data collection date corresponded with the dates of our NPP ground measurements.

5.1 Landsat ETM+ Data And Registration

Figure 1 shows Landsat ETM+ path 131, row 028, 30 m spatial resolution data acquired on June 12, 2001. To align the NPP measurement points with the satellite data, we measured latitude and longitude at recognizable points (such as the airport) and selected ground control points (GCP) on the satellite image. A GPS-IIIplus (GARMIN) and a LandMaster GPS camera (Konia) with WGS84 (World Geodetic System 1984) were used to determine the ground coordinates.

Japan has many points (such as water features and paved roads) that appear on satellite imagery and make GCP determination relatively easy. However, the study site in Mongolia lacked buildings and paved roads, making GCP determination difficult. We thus used the nearby town and an intersection on the way to town as GCPs. Once the GCPs were determined, affine conversion was performed, creating less than 10 m registration difference in all directions.

5.2 PAR And Air Temperature In June 2001

We measured global solar irradiance at the Mongolian Plateau site in 2001. Figure 5 shows the PAR calculated from global solar irradiance.

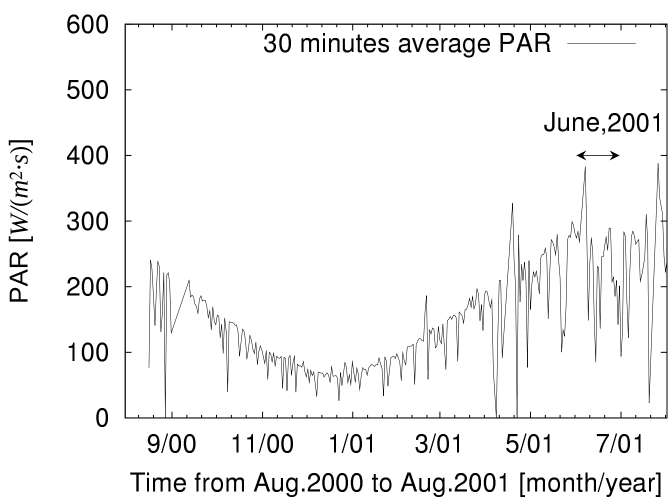

Figure 5. PAR calculated from global solar irradiance at Mandalgovi, Mongolia.

Monthly average PAR was calculated using the average of 13 sunlit hours (from 7:30 to 20:30). The resulting PAR of 230 $[W/m^2]$, representing June 1-30, 2001, included rainy, cloudy, and clear days.

To estimate vegetative respiration (R_d), we used monthly average air temperature expressed in equation (9). Figure 6 shows the air temperature measured at the study site from September 2000 to July 2001.

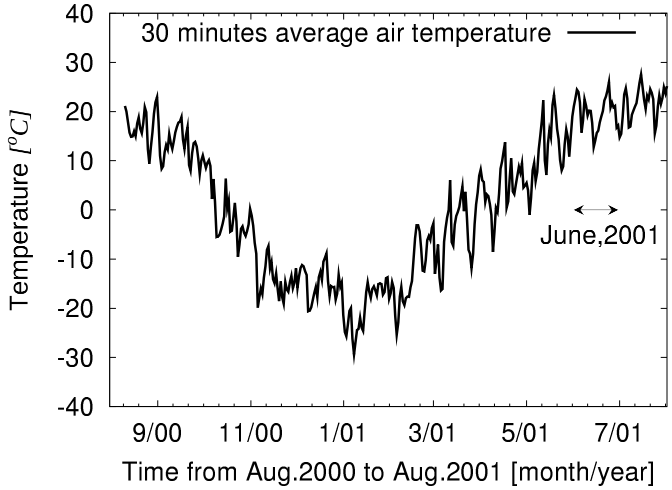

Figure 6. Air temperature at Mandalgovi, Mongolia.

In June 2001, the average monthly air temperature was 20[° C].

5.3 Results And Discussion

To understand $VIPD$ characteristics in the Mongolian Plateau, we calculated the $VIPD$ from the sample area using Landsat ETM+ data from June 12, 2001. The $VIPD$ values of water, soil, and four NPP ground measurement areas (areas ALM3, CRG, C2, and ALM4) were -0.101, -0.079, 0.065, 0.048, 0.048, and 0.049, respectively. We also calculated $VIPD$ for a temperate forest in Japan using Landsat ETM+ data from June. The temperate forest measurements resulted in a value of 0.805. Table 4 summarizes these results.

Table 4. $VIPD$ calculated for sample areas.

Water	Soil	ALM3	CRG	C2	ALM4	Japanese forest
-0.101	-0.079	0.065	0.048	0.048	0.049	0.805

The Mongolian Plateau's sparse vegetation can also be measured using satellite sensor data to create a $VIPD$. However, the $VIPD$ for Mongolia was much lower than that for temperate forests in Japan.

Table 5 shows the NPP estimated by equation (11) for the four study areas. Sites ALM3, CRG, C2, and ALM4 had estimated NPP of 0.052±0.014, 0.038±0.010, 0.038±0.010, and 0.038±0.010 $[kgCO_2/(m^2 \cdot month)]$, respectively. Propagation of error techniques (Bevington et al. 1992) revealed an approximately ±26% error of estimation in the estimated NPP. This error figure included the error in calculating PAR from global solar irradiance and the error in estimating GPP from average PAR during sunlit hours.

Table 5. NPP estimation at the four study areas in June 2001.

	ALM3	CRG	C2	ALM4
$[kgCO_2/(m^2 \cdot month)]$	0.052±0.014	0.038±0.010	0.038±0.010	0.038±0.010

Next, we compared NPP values derived from satellite data and ground measurements at the four study sites. Table 1 shows the ground-measured NPP that we compared to the estimated NPP shown in Table 5. Figure 7 shows the results of this comparison.

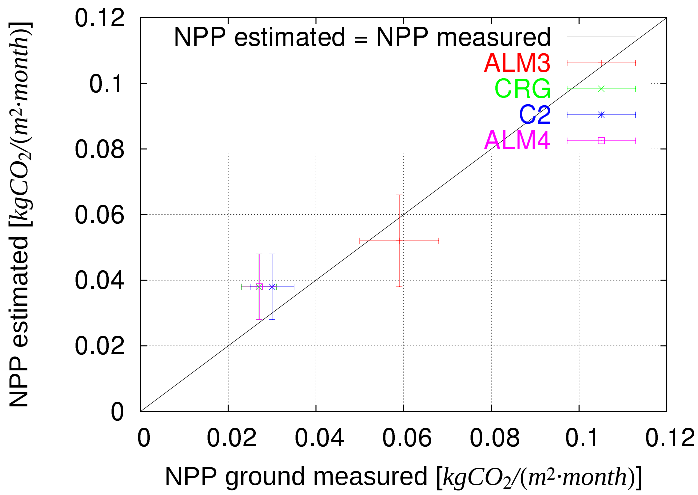

Figure 7. Estimated and measured NPP.

The NPP estimated from June 2001 Landsat ETM+ data matched the NPP measured in June 2001 at the Mongolian Plateau study sites within an acceptable range of error.

6 CONCLUSIONS

We measured above-ground NPP for the Mongolian Plateau study sites to verify the NPP estimation algorithm developed from data on temperate vegetation in Japan. We also collected Mongolian Plateau weather data required for NPP estimation, including global solar irradiance, PAR, and air temperature. Of these data, daily averaged PAR during sunlit hours was effective for NPP estimation.

We estimated the NPP of an area in Mongolia with low vegetation density by using Landsat ETM+ data. The average estimated NPP was 0.056 ± 0.015 $[kgCO_2/(m^2 \cdot month)]$ at our $60km \times 60km$ study area. The NPP estimated by using satellite data agreed with ground measurement data from the four Mongolian study sites within a ground measurement error of 15%.

This research shows that the NPP estimation algorithm we developed could be applied to semi-arid areas such as Mongolia. In the future, we plan to use the algorithm to estimate global NPP from satellite data.

ACKNOWLEDGMENTS

We thank the members of Ishida Laboratory for assistance with this research and for lending us the single-leaf photosynthesis equipment and the portable automatic leaf microclimate control system LCA-4 (Analytical Development Co. Ltd.) used for this research.

We are also deeply grateful to Professor Furukawa of the Biology Department of Nara Women's University for his valuable advice.

This study is part of the ADEOS-II/AMPEX-AMSR/AMSR-E project and the ADEOS-II/GLI project supported by the National Space Development Agency (NASDA), Japan. This project was conducted in partnership with the Institute of Meteorology and Hydrology, Ministry of Nature and Environment, Mongolia.

REFERENCES

BEVINGTON, P. R., and ROBINSON, D. K., 1992, Data reduction and error analysis for the physical sciences. 41-50.

CHANG, J. H., 1968, The agricultural potential of the humid tropics. *The geographical review*, **58**, 3, 333–361.

CHOUDHURY, B. J., 1987, Relationships between vegetation indices, radiation absorption, and net photosynthesis evaluated by a sensitivity analysis. *Remote Sensing of Environment*, **22**, 209–233.

DAIGO, M., ONO, A., URABE R., and FUJIWARA, N., in press, Pattern decomposition method for hyper-multispectral data analysis. *International Journal of Remote Sensing.*

FUJIWARA, N., MURAMATSU, K., AWA, S., HAZUMI, T., and OCHIAI, F., 1996, Pattern expansion method for satellite data analysis (in Japanese). *Journal of the Remote Sensing Society of Japan*, **16(3)**, 17–34.

FURUMI, S., HAYASHI, A., MURAMATSU, K., and FUJIWARA, N., 1998, Relation between vegetation vigor and a new vegetation index based on the pattern decomposition method. *Journal of the Remote Sensing Society of Japan*, **18(3)**, 17–34.

FURUMI, S., XIONG, Y., and FUJIWARA, N., submitted, Using multi-spectral data and ground measurements to estimate canopy photosynthesis by the pattern decomposition method. *Journal of the Remote Sensing Society of Japan.*

GOWARD, Samuel N., and DYE, Dennis G., 1987, Evaluating North American net primary productivity with satellite observations. *Adv. Space Res.*, **Vol. 7, No. 11**, 165–174

HAYASHI, A., MURAMATSU, K., FURUMI, S., SHIONO, Y., and FUJIWARA, N., 1998, An algorithm and new vegetation index for ADEOS-II/GLI data analysis. *Journal of the Remote Sensing Society of Japan*, **18(2)**, 28–50.

KAIHOTSU, I. (Principal Investigator), 2000, Ground Truth Evaluations of AMSR and GLI Soil Moisture and Geophysical/Vegetation Parameters Related to Ground Surface Conditions in the Mongolian Plateau. *NASDA-JRA.*

MAISONGRANDE, P., RUIMY, A., DEDIEU, G., and SAUGIER, B., 1995, Monitoring seasonal and inter-annual variations of gross primary productivity, net primary productivity, and net ecosystem productivity using a diagnostic model and remotely-sensed data. *Tellus*, **47B**, 178–190.

Monteith, J. L., 1981, Climatic variation and the growth of crops. *Quarterly Journal of the Royal Meteorological Society*, **107**, 749–774.

Muramatsu, K., Awa, S., Hayashi, A., Fujiwara, N., Daigo, M., and Ochiai, F., 1998, Pattern decomposition method in the albedo space for Landsat/TM and MSS data analysis. *International Journal of Remote Sensing*, **21(1)**, 99–119.

Nomoto, K., and Yokoi, Y., 1981, Shokubutsu no bushitsu seisan (Primary production by vegetation).